Two-detector Doppler broadening study of enhancement in Al

1998 J. Phys.: Condens. Matter 10 10383

(http://iopscience.iop.org/0953-8984/10/46/005)

J. Phys.: Condens. Matter **10** (1998) 10383–10390. Printed in the UK PII: S0953-8984(98)97567-1

Two-detector Doppler broadening study of enhancement in Al

P E Mijnarends†, A C Kruseman†, A van Veen†, H Schut† and A Bansil‡

† Interfaculty Reactor Institute, Delft University of Technology, 2629 JB Delft, The Netherlands

‡ Department of Physics, Northeastern University, Boston, MA 02115, USA

Received 30 April 1998

Abstract. Enhancement due to positron–electron correlation has been studied in Al by calculating and measuring Doppler profiles and positron lifetimes. It is found that only the local density enhancement of Puska, Seitsonen and Nieminen can simultaneously reproduce the profile and the lifetime, but our analysis suggests that a GGA-type enhancement of reduced strength would likely give even better results.

1. Introduction

The Doppler broadening method plays an important role in the application of positron annihilation spectroscopy to the study of defects in materials [1]. The longitudinal component p_L of the positron–electron (e^+–e^-) momentum along the direction of emission of one of the annihilation photons gives rise to a Doppler shift $\Delta E = \pm p_L c/2$ in the photon energy. Since both positive and negative shifts occur, the result is a broadening by an amount $2\Delta E = p_L c$ of the 511 keV line which is measured with a solid state detector. Owing to background problems only annihilations with valence electrons and low-momentum core electrons can be measured reliably.

In 1977 Lynn *et al* added a second Ge(Li) detector to the Doppler broadening setup in order to observe the second annihilation photon in coincidence [2]. This resulted in an improvement of the peak to background ratio by two orders of magnitude and of the energy resolution by a factor of $\sim \sqrt{2}$. As a result it became possible to observe high-momentum annihilations with the core electrons without being hampered by the background. Recently this method, dormant for many years, has been revived [3, 4] and it has been demonstrated that its elemental specificity can be employed in the identification of impurity atoms bound to vacancies [5].

The wide momentum range accessible by the two-detector method enables one to observe the effects of e^+-e^- correlation over a wide range of electron densities, from the high-density core to the relatively low-density interstitial region. This is not only of particular importance in the study of defects where e^+-e^- correlation affects the annihilation of trapped positrons, but also in perfect metals since these serve as a testing ground. A scheme developed to describe e^+-e^- correlation should therefore in the first place yield correct results in perfect metals.

In the present study we have employed the two-detector Doppler broadening method to study the validity of three schemes for incorporating e^+–e^- correlation into the calculation of the momentum density in aluminium. A proper calculation should correctly predict *both*

0953-8984/98/4610383+08$19.50

the e^+ lifetime and the momentum distribution. Aluminium was chosen because earlier calculations using two of these schemes have yielded lifetimes significantly shorter than experiment, although one of them was able to reproduce the momentum density [6]. In the present paper new experimental lifetime and Doppler profile data are presented, and it will be shown that the third scheme is able to explain this body of data in a reasonably satisfactory manner.

2. Experimental procedure

2.1. Technique

In a two-detector Doppler broadening experiment the count rate is a function of the measured energies E_1 and E_2 of the two photons. A histogram in the E_1, E_2 plane (figure 1) shows a roughly elliptical profile with its major axis along the line $E_2 = 2m_0c^2 - E_B - E_1$, stemming from positrons undergoing two-photon annihilation in the sample. Here, m_0c^2 is the rest energy of each of the annihilating particles and E_B the binding energy of the particle pair. Weak ridges along the lines $E_1 = 511$ keV and $E_2 = 511$ keV are due to accidental coincidences. The high-energy parts of these (i.e., beyond 511 keV) involve cosmic rays or pile-up events; the low-energy parts are due to incomplete charge collection in one of the detectors and to Compton scattering. The crest of the three-dimensional profile yields the well-known Doppler profile with a superior signal to background ratio (10^5 : 1). If the resolution of the two detectors were ideal, a cross section through the profile along the line $E_2 = E_1$ would yield a δ function. In reality, a peak is obtained with a finite width

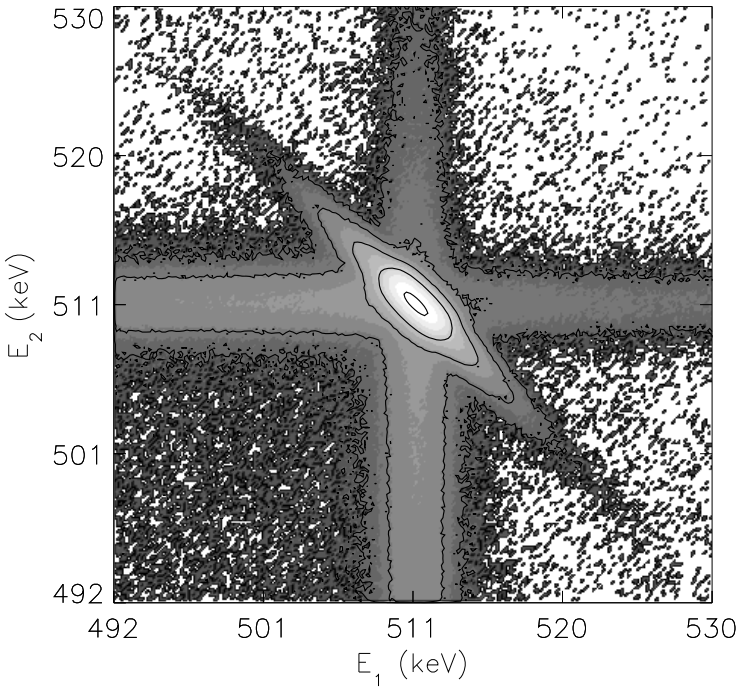

Figure 1. Distribution of coincident Doppler events as a function of the measured energies E_1 and E_2. Contours increase by a factor of 10.

representative of the resolution of the setup. This peak is made up of contributions from all groups of electrons taking part in the annihilation process. Thus, the peak consists of a sum of a number of peaks, each one displaced by half the binding energy of the corresponding electron shell, with a width given by the instrumental resolution and an intensity determined by the wavefunction overlap between the positron and the electrons in that shell.

2.2. Doppler profile

22 keV positrons from the slow-positron beam at Delft were made to impinge on an Al single crystal, orientated with a [110] axis along the e^+ beam and a [001] axis along the line connecting the two Ge detectors in coincidence, placed at 3.5 cm on either side of the sample. Another measurement was performed with this distance increased to 25 cm to ascertain that the data were not affected by the large solid angle subtended by the detectors. Figure 2 shows the Doppler profile for Al. The e^+ lifetime, measured in a separate setup, was 164 ± 2 ps, in good agreement with the value of 163 ps quoted by Schaefer *et al* [7].

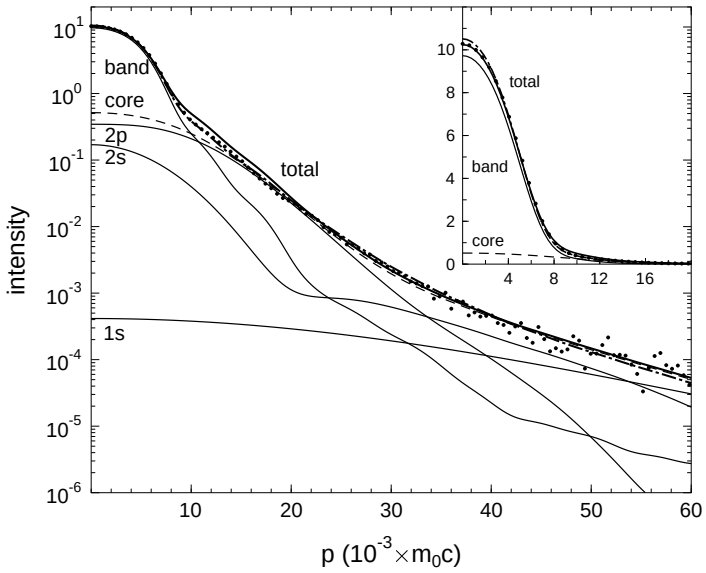

Figure 2. Calculated LDA′ (solid curves; the dashed curve gives the total core contribution), GGA (chain curve) and measured Doppler profiles in Al with $\boldsymbol{p}$ along the [100] direction. The inset shows the low-momentum region on a linear scale. All curves are normalized to the calculated (LDA′) lifetime of 166 ps.

While a mapping of the well known shape parameters W versus S provides insight into the defect population of a material [8], the detailed shape of the profile itself yields information on e^+–e^- correlation. A positron in a gas of electrons attracts a cloud of electrons which screens the positive charge of the positron. Thus, the electron density 'seen' by the positron is higher than the average density of the electrons—an effect called enhancement. As a result, the lifetime of the positron will be shortened with respect to the Sommerfeld value, and the momentum density of the e^+–e^- pairs, and thus the shape of the Doppler profile, will be affected. This point will be investigated more closely in section 4 by comparing the experimental profile with the results of calculations using various forms of enhancement.

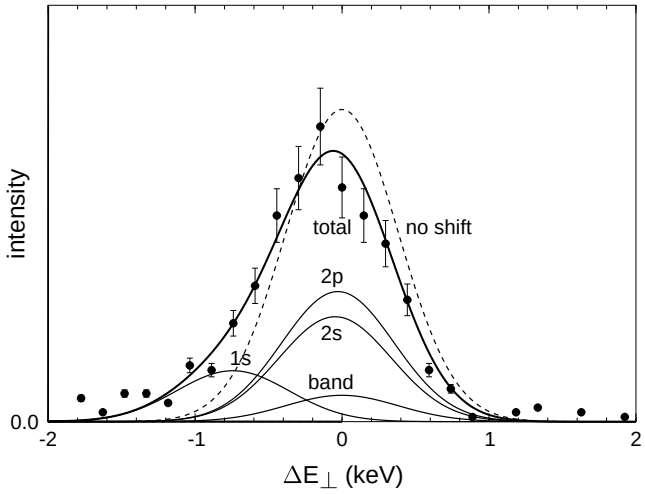

Figure 3. Measured and calculated (with LDA′ enhancement) cross section of the Doppler distribution in figure 1 at $\Delta E = 9$ keV.

2.3. Binding energy

Figure 3 shows a measured cross section of the Doppler distribution in figure 1, parallel to the line $E_1 = E_2$ at a momentum of $35 \times 10^{-3} m_0 c$ which corresponds to $\Delta E = 9$ keV (a momentum of $10^{-3} m_0 c$ corresponds to an angle of 1 mrad in an angular correlation experiment). Also shown are the contributions of the various groups of electrons and the total profile calculated with the LDA′ enhancement (see below). The largest contribution comes from the 2p and 2s electrons while there are smaller contributions from the 1s and band electrons. The 2p and 2s peaks are marginally shifted with respect to the centre of the peak of the conduction electrons, the binding energies for these shells being 57 and 94 eV, respectively. Farther out in the tail the contribution of the 1s electrons can be seen (at $\Delta E_\perp = \frac{1}{2} E_B = -0.744$ keV, where $\Delta E_\perp$ is defined by $E_{1(2)} = 511$ keV $+(-)\Delta E + \Delta E_\perp$). Addition of these contributions yields a curve with a small but noticeable skewness. The calculated solid curve in figure 3 is seen to be in fair agreement with the experimental data, contrary to the dashed curve which does not include the binding energy. From a similar cross section taken at $E_1 = E_2 = 511$ keV along the line $E_1 = E_2$ (where the core electrons play only a minor role), the energy resolution of the setup is found to be 0.90 keV.

3. Calculations

3.1. Electronic structure

In the present study we have employed the KKR-based methodology [9]–[11] used successfully in high-T_c and other materials [12]. In the independent particle model the momentum density for positrons with wavefunction ϕ_+ annihilating with an electron with wavefunction ψ_j is defined by

$$\rho^{2\gamma}(\boldsymbol{p}) = \sum_j \left| \int \mathrm{e}^{\mathrm{i}\boldsymbol{p}\cdot\boldsymbol{r}} \psi_j(\boldsymbol{r}) \phi_+(\boldsymbol{r}) \, \mathrm{d}\boldsymbol{r} \right|^2 \tag{1}$$

where the summation runs over all occupied electron states. In the KKR formalism the contribution of the band electrons is given by the following expression [13] (for one atom per unit cell of volume Ω and a positron in its ground state $\boldsymbol{k}_+ = 0$)

$$\rho^{2\gamma}(\boldsymbol{p}) = \frac{(4\pi)^4}{\Omega^2} \sum_{E_j<E_F} \left| \sum_n \sum_{LL'} \overline{C}_L(\boldsymbol{k}) \frac{S_L(\boldsymbol{p}-\boldsymbol{K}_n, E)}{E-|\boldsymbol{p}-\boldsymbol{K}_n|^2} \overline{C}^+_{L'} \frac{S^+_{L'}(\boldsymbol{K}_n, E_+)}{E_+ - K_n^2} \right|^2 \times \left(\sum_{LL'} \overline{C}^*_L(\boldsymbol{k})\, \dot{M}_{LL'}\, \overline{C}_{L'}(\boldsymbol{k}) \sum_{\Lambda\Lambda'} \overline{C}^{+*}_{\Lambda}\, \dot{M}^+_{\Lambda\Lambda'}\, \overline{C}^+_{\Lambda'} \right)^{-1} \Bigg|_{E=E_j}. \tag{2}$$

In this equation '+' labels positron quantities, $\overline{C}_L = \kappa \cot \eta_l C_L$, where L denotes the quantum numbers (l, m), $\kappa = E^{\frac{1}{2}}$, $\eta_l(E)$ is the lth scattering phase shift, and the C_L are the coefficients in the KKR trial wavefunction for wavevector $\boldsymbol{k}$ and energy E:

$$\psi_{\boldsymbol{k},E}(\boldsymbol{r}) = \sum_L i^l C_L(\boldsymbol{k}, E) R_l(r, E) Y_L(\hat{\boldsymbol{r}}). \tag{3}$$

$\dot{M}_{LL'} = \mathrm{d}M_{LL'}/\mathrm{d}E$ is the energy derivative of the (LL') element of the KKR matrix M, and the quantity $S_L(\boldsymbol{p}, E)$ is given by

$$S_L(\boldsymbol{p}, E) = -\kappa \cot \eta_l Y_L(\hat{\boldsymbol{p}}) \int_0^{r_i} j_l(pr) V(r) R_l(r, E) r^2 \,\mathrm{d}r \tag{4}$$

where $V(r)$ is the muffin-tin potential, j_l is a spherical Bessel function, Y_L is a spherical harmonic, and r_i is the radius of the muffin-tin sphere. Equation (2) has the form of a convolution and does not assume spherical symmetry of the e^+ wavefunction.

3.2. Enhancement

In the present study we have employed three enhancement schemes based on local density theory. The first one, designated LDA, is derived from the many-body results of Arponen and Pajanne [14]. The parametrization of their results by Boroński and Nieminen [15] produces a simple expression for the e^+–e^- correlation energy (described by a correlation term V_c in the e^+ crystal potential). Barbiellini *et al* [16] have parametrized the enhancement factor γ in a way consistent with the correlation energy. Both expressions are functionals of the local electron density $n(\boldsymbol{r}) = 3/(4\pi r_s^3)$. The second one, termed LDA′, is based on the hypernetted chain computations of Lantto [17] and has been parametrized by Puska *et al* [18]. This LDA′ enhancement factor is weaker than the one in the LDA scheme over most of the cell, as illustrated by figure 4 for aluminium. The third scheme takes into account that the e^+–e^- correlation may not be a function of the local electron density alone, but also of its gradient. In this generalized gradient approximation (GGA) proposed by Barbiellini *et al* [16] the correlation potential and the enhancement factor are given by

$$V_c^{\mathrm{GGA}} = V_c^{\mathrm{LDA}}\, \mathrm{e}^{-\alpha\epsilon/3} \tag{5}$$

$$\gamma^{\mathrm{GGA}} = 1 + (\gamma^{\mathrm{LDA}} - 1)\, \mathrm{e}^{-\alpha\epsilon} \tag{6}$$

respectively, where

$$\epsilon = |\nabla n|^2/(n q_{\mathrm{TF}})^2 = |\nabla \ln n|^2/q_{\mathrm{TF}}^2 \tag{7}$$

and $1/q_{\mathrm{TF}}$ denotes the Thomas–Fermi screening length and α is a constant chosen such that the experimental and theoretical e^+ lifetimes agree as well as possible. The choice $\alpha = 0.22$ appears to give a good general agreement for a large number of solids [16]. For a uniform electron gas $\epsilon = 0$ and $\gamma^{\mathrm{GGA}} = \gamma^{\mathrm{LDA}}$, while in the core region, where the electron density changes rapidly, ϵ becomes large and γ^{GGA} approaches 1, i.e., there is no enhancement. The

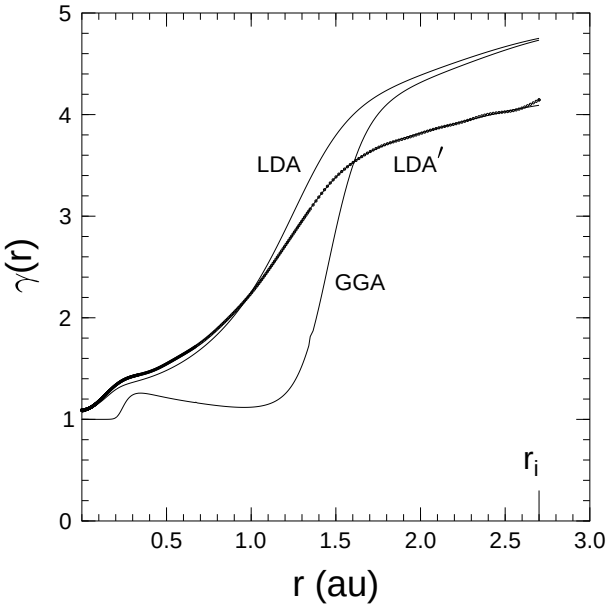

Figure 4. Enhancement factor $\gamma[n(\boldsymbol{r})]$ (solid curves) in the muffin-tin sphere in Al for different models of enhancement. The dots which (except close to the muffin radius r_i) coincide with the LDA′ curve give the Fourier series representation of that curve.

curve for γ^{GGA} in figure 4 reflects the shell structure of the core electrons and shows that the GGA enhancement is close to 1 in the core region.

The annihilation rate λ of a positron with the electrons in a solid (which equals the inverse of the e^+ lifetime τ) is given by

$$\lambda = \pi r_e^2 c \int n(\boldsymbol{r})|\phi_+(\boldsymbol{r})|^2 \gamma[n(\boldsymbol{r})]\,\mathrm{d}\boldsymbol{r} \tag{8}$$

which, after Fourier transformation, can also be written as

$$\lambda = \frac{\pi r_e^2 c}{(2\pi)^3} \int \rho^{2\gamma}(\boldsymbol{p})\,\mathrm{d}\boldsymbol{p} \tag{9}$$

where r_e denotes the classical electron radius. It is then consistent with equation (8) to write the momentum density $\rho^{2\gamma}(\boldsymbol{p})$ as

$$\rho^{2\gamma}(\boldsymbol{p}) = \sum_j \left| \int \mathrm{e}^{\mathrm{i}\boldsymbol{p}\cdot\boldsymbol{r}} \psi_j(\boldsymbol{r})\phi_+(\boldsymbol{r})\sqrt{\gamma[n(\boldsymbol{r})]}\,\mathrm{d}\boldsymbol{r} \right|^2. \tag{10}$$

The core contribution is calculated assuming that the positron wavefunction is spherically symmetric in the region around each nucleus where the core electron density is appreciable. When there is degeneracy with respect to the magnetic quantum number m, the various core contributions can be written as

$$\rho_{nl}^{2\gamma}(\boldsymbol{p}) = 4\pi(2l+1) \left| \int j_l(pr) R_{nl}(r) R_+(r) r^2 \sqrt{\gamma(r)}\,\mathrm{d}r \right|^2 \tag{11}$$

where R_{nl} and R_+ are the radial parts of the electron and positron wavefunctions, respectively, and j_l is the spherical Bessel function. Finally, the Doppler profile is obtained by integrating $\rho^{2\gamma}(\boldsymbol{p})$ with respect to the two transversal components of $\boldsymbol{p}$.

4. Results and discussion

The electronic structure of core and conduction electrons in aluminium ($a = 0.4050$ nm) has been calculated self-consistently at 489 $\boldsymbol{k}$ points in 1/48th of the Brillouin zone. The valence electron wavefunctions include spherical waves up to and including $l = 3$. The iterations were based on 1800 $\boldsymbol{k}$ points in the irreducible wedge, and the final potential was stable to within 0.5 meV. Attention was paid to convergence of all parts of the calculation. The e^+ eigenvalue and wavefunction at $\boldsymbol{k} = 0$ were obtained for the GGA and the two LDA schemes using the appropriate correlation potentials. The GGA positron state was found to lie 0.14 eV higher than in the LDA. The enhancement factor $\sqrt{\gamma}$ was introduced into equation (1) by expanding it into a Fourier series of 16000 $\boldsymbol{K}$ vectors ($\sqrt{\gamma}$ has the lattice periodicity) and convoluting this series with that for the positron, thus yielding an effective e^+ wavefunction $\sqrt{\gamma(\boldsymbol{r})}\,\phi_+(\boldsymbol{r})$. The total momentum density $\rho^{2\gamma}(\boldsymbol{p})$ was calculated at $\sim 6 \times 10^7$ $\boldsymbol{p}$ points on a $385 \times 385 \times 385$ uniform mesh of $\Delta p = 0.374 \times 10^{-3} m_0 c$. Tests showed that 1989 plane waves for the positron were sufficient to ensure convergence of the band electron momentum density up to $70 \times 10^{-3} m_0 c$; for the 2s and 2p contributions 7943 plane waves were used. The 1s contribution was calculated using (11).

Table 1. Positron lifetime τ using different enhancement schemes.

LDA	GGA	LDA′	Experiment
144 ps	153 ps	166 ps	164 ± 2 ps

Firstly, the positron lifetime was calculated using (9); the results are listed in table 1. The LDA and the GGA calculations, both based on the parametrized Arponen–Pajanne theory, yield a lifetime significantly shorter than experiment. These lifetimes agree with the values given by Barbiellini *et al* [16] based on LMTO computations and suggest that in Al the enhancement resulting from the Arponen–Pajanne theory is too high, even when gradients in the electron density are taken into account. The LDA′ value of 166 ps, on the other hand, is in reasonably good agreement with experiment and shows that a somewhat reduced enhancement produces the correct lifetime.

Figure 2 shows a comparison between the experiment and a computation of the Doppler profile using the LDA′. It also contains the total profile calculated using the state-dependent form [19] of the GGA. All calculated curves have been convoluted with the experimental resolution of 0.90 keV. The LDA′ curve fits the experiment very well except in the range between 10 and $20 \times 10^{-3} m_0 c$. The GGA curve provides a better fit in this range owing to its lower core enhancement. At low momenta, however, the GGA curve is too high. This, together with the too short lifetime of 153 ps, suggests that γ^{GGA} is somewhat too high in the outer part of the cell. A GGA-type enhancement factor rising to a value intermediate between that of GGA and LDA′ might well be able to simultaneously reproduce the measured lifetime and yield an accurate fit to the experimental profile over the entire momentum range.

Finally, it is interesting to note that the excellent fit at high momenta (say, 40 to $60 \times 10^{-3} m_0 c$) is due to the use of solid state 2s and (particularly) 2p band wavefunctions. If atomic core wavefunctions are used the core contribution at high momenta is higher, which worsens the fit with experiment. The crystalline environment affects the 2s and 2p electrons and gives these levels 'bandwidths' of 3.8 and 23 meV, respectively.

In summary, it has been shown by using the two-detector Doppler broadening method

that among the various enhancement schemes in use the LDA′ scheme is so far the only one that yields a positron lifetime and a Doppler profile for Al that are both in reasonably good agreement with experiment. A somewhat weaker GGA enhancement, however, might take away the residual difference in the Umklapp region. These tests should be extended to other metals.

Acknowledgments

This work is sponsored by the National Computer Facilities Foundation (NCF) for the use of supercomputer facilities with financial support from the Netherlands Organization for Scientific Research (NWO). It is also supported by the US Department of Energy under contract W-31-109-ENG-38, including a subcontract to Northeastern University, and benefited from the allocation of supercomputer time at NERSC and at the San Diego Supercomputer Center. We gratefully acknowledge a NATO travel grant.

References

[1] MacKenzie I K 1969 *Phys. Lett.* **30A** 115
[2] Lynn K G, MacDonald J R, Boie R A, Feldman L C, Gabbe J D, Robbins M F, Bonderup E and Golovchenko J 1977 *Phys. Rev. Lett.* **38** 241
[3] Alatalo M, Kauppinen H, Saarinen K, Puska M J, Mäkinen J, Hautojärvi P and Nieminen R M 1995 *Phys. Rev.* B **51** 4176
[4] Matsui S 1992 *J. Phys. Soc. Japan* **61** 187
[5] Asoka-Kumar P, Alatalo M, Ghosh V J, Kruseman A C, Nielsen B and Lynn K G 1996 *Phys. Rev. Lett.* **77** 2097
[6] Barbiellini B, Puska M J, Alatalo M, Hakala M, Harju A, Korhonen T, Siljamäki S, Torsti T and Nieminen R M 1997 *Appl. Surf. Sci.* **116** 283
[7] Schaefer H-E, Gugelmeier R, Schmolz M and Seeger A 1987 *Mater. Sci. Forum* **15–18** 111
[8] Van Veen A, Kruseman A C, Schut H, Mijnarends P E, Kooi B J and De Hosson J Th M 1997 *Mater. Sci. Forum* **255–257** 76
[9] Kaprzyk S and Bansil A 1990 *Phys. Rev.* B **42** 7358
[10] Bansil A and Kaprzyk S 1991 *Phys. Rev.* B **43** 10335
[11] Bansil A, Kaprzyk S and Toboła J 1992 *Applications of Multiple Scattering Theory to Materials Science* ed W H Butler *et al* (Pittsburgh: MRS)
[12] Bansil A, Pankaluoto R, Rao R S, Mijnarends P E, Długosz W, Prasad R and Smedskjaer L C 1988 *Phys. Rev. Lett.* **61** 2480
Bansil A, Mijnarends P E and Smedskjaer L C 1990 *Physica* C **172** 175
Pankaluoto R, Bansil A, Smedskjaer L C and Mijnarends P E 1994 *Phys. Rev.* B **50** 6408
[13] Mijnarends P E and Bansil A 1995 *Positron Spectroscopy of Solids* ed A Dupasquier and A P Mills Jr (Amsterdam: IOS) p 25
[14] Arponen J and Pajanne E 1979 *Ann. Phys., NY* **121** 343
[15] Boroński E and Nieminen R M 1986 *Phys. Rev.* B **34** 3820
[16] Barbiellini B, Puska M J, Torsti T and Nieminen R M 1995 *Phys. Rev.* B **51** 7341
[17] Lantto L 1987 *Phys. Rev.* B **36** 5160
[18] Puska M J, Seitsonen A P and Nieminen R M 1995 *Phys. Rev.* B **52** 10947
[19] Alatalo M, Barbiellini B, Hakala M, Kauppinen H, Korhonen T, Puska M J, Saarinen K, Hautojärvi P and Nieminen R M 1996 *Phys. Rev.* B **54** 2397